Supplementary information for "The Macroscopic Growth Laws of Brain Metastases"

Beatriz Ocaña-Tienda[1]*, Julián Pérez-Beteta[1], David Molina-García[1], Juan Jiménez[1], Odelaisy León-Triana[1], Ana Ortiz de Mendivil[2], Beatriz Asenjo[3], David Albillo[4], Luís Pérez-Romasanta[5], Manuel Valiente[6], Lucía Zhu[6], Pedro García-Gómez[6], Elizabeth González-Del Portillo[5], Manuel Llorente[4], Natalia Carballo[4], Estanislao Arana[7], Víctor M. Pérez-García[1]*

[1]Mathematical Oncology Laboratory, University of Castilla-La Mancha, Ciudad Real, Spain; [2]Department of Radiology, Sanchinarro University Hospital, HM Hospitales, Spain; [3]Department of Radiology, Hospital Regional Universitario Carlos Haya, Málaga, Spain; [4]Radiology Unit, MD Anderson Cancer Center, Madrid, Spain; [5]Radiation Oncology Service, Salamanca University Hospital, Salamanca, Spain; [6]Brain Metastasis Group, Spanish National Cancer Research Centre (CNIO), Madrid, Spain; [7]Department of Radiology, Fundación Instituto Valenciano de Oncología, Valencia, Spain;

*Corresponding authors: Beatriz.Ocana@uclm.es & Victor.PerezGarcia@uclm.es

S1. Stochastic model

Stochastic mesoscopic model of tumor growth

To simulate tumor growth three cellular population were accounted: healthy cells, tumor cells and necrotic cells. Biological processes, namely cell division, death and migration were implemented similarly to model in [1], although a small modification was incorporated in the tumor death process to reproduce specific characteristics observed in brain metastases.

The probabilistic events for this process reads as follows

$$P_{\text{Trep}} = \frac{\triangle x}{\tau_{\text{Trep}}}\left(1-\frac{n_t+n_n+n_h}{K}\right), \tag{S1}$$

$$P_{\text{Tmig}} = \frac{\triangle x}{\tau_{\text{Tmig}}}\left(\frac{n_t+n_n+n_h}{K}\right), \tag{S2}$$

$$P_{\text{Tdeath}} = \frac{\triangle x}{\tau_{\text{Tdeath}}}\left(\tanh\left(\frac{10(n_t+n_n+n_h-K_{\text{act}})}{K}\right)\right), \tag{S3}$$

$$P_{\text{Hmig}} = \frac{\triangle x}{\tau_{\text{Hmig}}}\left(\tanh\left(\frac{10(n_t+n_n+n_h-0.45K)}{K}\right)\right), \tag{S4}$$

where n_t, n_n and n_h denotes the number of total tumor cells, necrotic cells and healthy cells inside a given voxel, respectively. Parameters τ represent the characteristic times of each process and K_{act} is the local threshold of voxel capacity from which tumor cells begin to die due to lack of resources.

Then, the total numbers of proliferating and dying cells from tumor population are drawn from binomial distributions $B(n_t, P_{\text{Trep}})$ and $B(n_t, P_{\text{Tdeath}})$, respectively. Due to the acquired capacity of tumor cells to evade apoptosis [2], we will assume that apoptosis signaling is activated once 75% of the voxel limit carrying capacity (K_{act}) is exceeded, simulating a significant lack of resources for the tumor cells. This is explained in the probability of death P_{Tdeath} by the term of the hyperbolic tangent as a function of the voxel capacity. The number of migrating cells is also drawn from the respective binomial distribution $B(n_t, P_{\text{Tmig}})$ and then they are distributed around a neighborhood of 26 voxels (Moore neighborhood) according to a multinomial distribution [1]. For simplicity we have assumed all tumor cells comes from the same clonal population without including mutation events.

For healthy cells we assume that the levels of cell division and death remain in balance due to the ability of these cells to self-regulate, and that the biological process of migration is the only one that is affected by the evolution of tumor cells.Therefore, the numbers of migrating healthy cells is drawn from the binomial distribution $B(n_h, P_{\text{Hmig}})$ being displaced by the pressure performed by the tumor cells colonization when the total number of cells in the voxel exceeds 45% of its maximum capacity. Figure S1 is a slice of an actual simulation, where the colors indicate the voxel occupation. Each voxel contains a variable number of cells as described in the updating algorithm above.

Stochastic mesoscopic model of response to radiosurgery

When tumors are treated with radiosurgery, tumor cells are lethally damaged or killed due to high doses of radiation. In addition, a fraction of the surrounding healthy tissue can also be damaged. As a consequence, the immune system is activated and immune cells move to the irradiated region to repair the damage caused. To describe the response to this treatment we have included three new cell populations: damaged tumor cells, activated immune cells and damaged healthy cells.

The dynamics of these populations are given by the following probabilistic events:

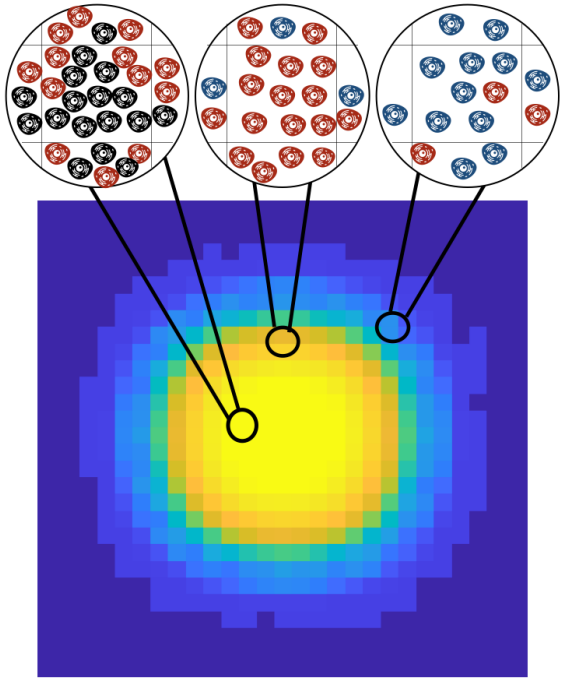

Figure S1 Slice of an actual simulation of tumor without treatment, with colors indicating occupation. Cells color indicates the different cell populations, with blue representing healthy cells, red representing tumor cells and black representing necrotic cells.

$$P_{Ddie} = \frac{\triangle x}{k \cdot \tau_{\text{Trep}}}, \tag{S5}$$

$$P_{\text{Iact}} = \frac{\triangle x}{\tau_{\text{act}}} \cdot \frac{n_n}{n_i} \left(1 - \frac{n_t + n_n + n_h + n_d + n_{hd} + q \cdot n_i}{K}\right), \tag{S6}$$

$$P_{\text{Ikill}} = \frac{\triangle x}{\tau_{\text{kill}}} \cdot \frac{n_i}{n_n} \left(1 - \frac{n_t + n_n + n_h + n_d + n_{hd}}{K}\right), \tag{S7}$$

$$P_{\text{Ideath}} = \frac{\triangle x}{\tau_{\text{Ideath}}}, \tag{S8}$$

$$P_{\text{Imig}} = \frac{\triangle x}{\tau_{\text{Imig}}} \left(\frac{n_t + n_n + n_h + n_d + n_{hd} + q \cdot n_i}{K}\right), \tag{S9}$$

where n_d, n_i and n_{hd} denote the number of total damaged tumor cells, activated immune cells and damaged healthy cells inside a given voxel, respectively. Similarly, parameters τ represent the characteristic times of each process and new cell populations are incorporated into the saturation process. Note that q is a scalar that normalizes the size of immune cells with respect to the size of healthy and tumor cells, assuming that the latter have similar sizes.

The number of damaged tumor cells are drawn from the binomial distribution $B(n_d, P_{Ddie})$. This cells population dies after the k cycle of mitosis while trying to repair the damage caused and then passes into the necrotic cell compartment. The number of necrotic cells that are eliminated by interaction with immune cells and the number of immune cells activated are drawn form the binomial distribution $B(n_n, P_{\text{Ikill}})$ and $B(n_i, P_{\text{Iact}})$, respectively. Further, the activated immune cells are removed naturally and this process is simulated form the binomial distribution $B(n_i, P_{\text{Ideath}})$. Analogous to tumor cells migration, the number of migrating immune cells is drawn from the binomial distribution $B(n_i, P_{\text{Imig}})$ using the same algorithm.

Therapy was implemented to resemble the actual radiosurgery in the experimental part of this study. To simulate the spatial distribution of radiation, we relied on the typical isodose plot for a Gamma Knife patient, as shown in Figure S2 A-B. In this example, the isodose surface that encloses the target (which is often taken as the prescription dose) is typically 50% of the maximum dose in the target. In addition, radiation doses (30% of the maximum dose) are also administered in a larger volume around the lesion, with an additional 1 to 2 mm diameter. This percentage may vary depending on the technique and machines used [3].

A single dose of SRS was simulated in-silico as follows: *i)* a fraction of tumor cells S_f will suffer either no damage and will remain viable, an additional fraction $(1 - S_f)$ will receive lethal damage of which a fraction ϵ will die on a short time scale (i.e. days), and the remainder will move into the compartment of lethally damaged cells; *ii)* a fraction of immune cells I_f will be activated and *iii)* a fraction of healthy cells surrounding the tumor H_f will suffer lethal damage. Figure S2C shows an example of the spacial distribution of cell population before and after SRS as described above.

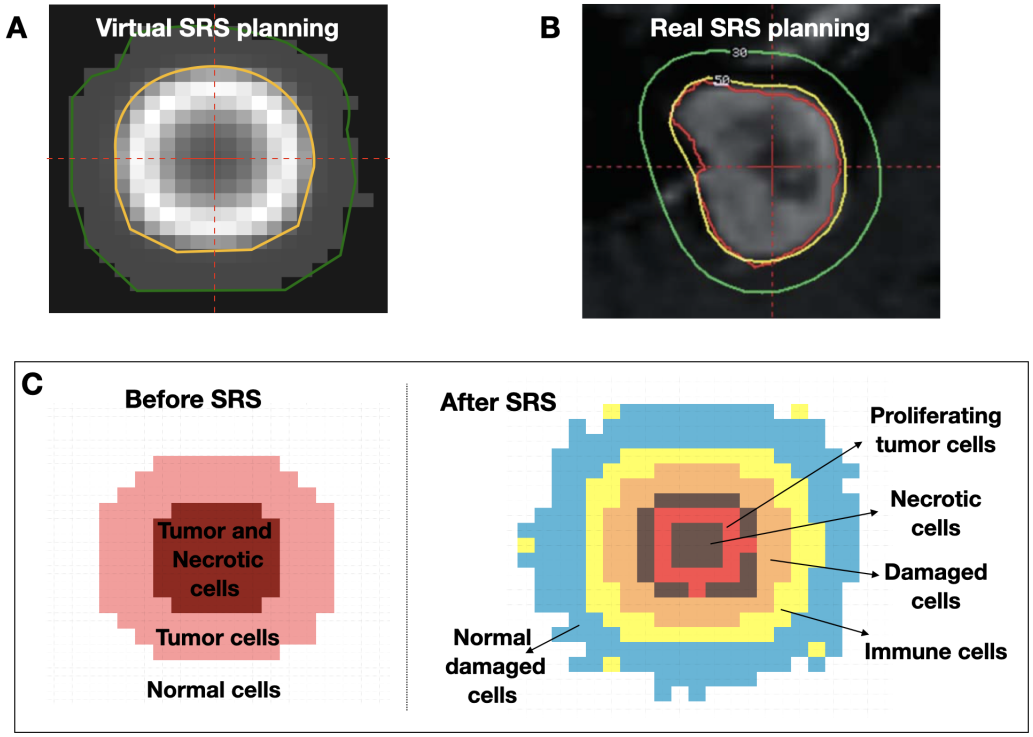

Figure S2 **A** A single-shot treatment plan for a vitual simuation of SRS treatment.The target is outlined in yellow, and it is the area most affected by SRS. The green line encloses another area affected with less intensity. **B** A real example of Gamma Knife isodose plot with the target outlined in red, the 50% isodose line in yellow, and the 30% isodose line in green. Figure adapted from [3]. **C** Spatial distribution of cell populations before and after SRS. The voxels can be occupied by more than one cell population but the colors per voxel of the representative samples of each population are shown.

Estimation of parameters

To fix the initial data we used the sizes typically found in the clinical setting for the tumor sizes pre-SRS treatment, which are around 0.5-2 cm^3 and the tumor maximum sizes until 10 cm^3. Hence, we selected L = 60 voxels per spatial length to make these sizes attainable. The time step was fixed to 4 hours. From typical cell sizes [4] we estimated the carrying capacity of a single voxel N_{max} to be 2×10^5 cells and we have assumed same size for all type of cells. The choice of division, death, and migration basal rates used the doubling times estimations [5] and imaging data from real BMs in [6].

Several studies indicated increased microglial activation, proliferation, and phagocytosis may contribute to onset of neuro-inflammation-induced brain injury. To estimate the parameters related with the immune system we have based on this cell population [7, 8]. Microglia are the resident macrophages of the brain, comprising 0.5%—16.6% of the total number of cells in the human brain [9]. For this reason, we set the initial number of immune cells as 10% of the healthy cells surrounding the tumor. Microglial activation is characterized by morphological changes, including an increase in size. There is great heterogeneity in the cell morphology of the microglia. Based on previous morphological studies [10] we assume that in the normal state microglia cells have the same size and in the activation state they present an increase of 50% in their size, hence the parameter $q = 3/2$ in the saturation process. Recent studies have reported the microglial landscape changes radically within a few weeks, with cells dying and other taking their place [9]. Thus, we take the mean lifetime of immune cells in a voxel to be around 2 months and activation to be in the range of 12-20 hours.

All the proposed parameters are associated with cellular processes, which combined result in whole-tumor rates. Cellular traits were randomly sampled from the range of allowed basal rates for each simulation. This provided variability between individual simulations and allowed us to assess the robustness of the model’s behavior.

Virtual BMs simulations

To simulate the tumor growth dynamics after SRS, we ran a set of 400 simulations of BMs starting from 10^3 tumor cells, allowing them to grow until reaching diagnostic volumes in the range of $0.5 - 2$ cm^3. Then, the radiosurgery event was simulated and post-treatment tumor evolution continued as described in Section 1. Each simulation had a different set of basal rates, sampled randomly from the ranges specified in Table S1. Because the large number of parameters in the model is sufficient to guarantee variability between the different tumor responses to treatment, the ranges of tumor proliferation and migration rates were reduced to 500h (±10) and 1000h (±10) respectively.

Furthermore, we assumed that radiosurgery achieves an initial reduction in the volume of the lesion. To do this, we used the following voxel survival fraction

Parameters	Meaning (average times per voxel)	Value (hours)
τ_{Trep}	Tumor cells reproduction	450-550
τ_{Tmig}	Tumor cells death	7000-1500
τ_{Tdeath}	Tumor cells migration	1000-2000
τ_{Imig}	Immune cells migration	150-250
τ_{Imig}	Immune cells death	1440- 1560
τ_{act}	Immune cells activation	12-20
τ_{kill}	Necrotic tumor cells elimination	72- 96
$\bar{\tau}_{\text{kill}}$	Necrotic healthy cells elimination and vascular repair	200- 280

Table S1 Relevant parameter values for the stochastic model.

$$S_f = S_{\hat{f}} \cdot \tanh\left(\frac{10(n_n - 0.45K)}{K}\right), \tag{S10}$$

where $S_{\hat{f}}$ is the maximum survival fraction. This expression is supported by the fact that well oxygenated cells are less resistant to radiation (more radio sensitive). Thus, the cells that are farthest away and that do not get enough oxygen and nutrients to survive are those that are found in the voxels with the highest number of necrotic cells.

The simulations were divided into two groups. First, a control group of 200 BM simulations was performed under the condition of not damage to the healthy tissue surrounding the tumor ($S_n = 1$). A second group of 200 BM simulations accounted for the damage induced by SRS to healthy tissue next to the lession ($0.1 \leq S_n \leq 0.7$). The latter would be the situation that was expected to occur in the clinics.

Calculation of β exponent for a virtual tumor

We focused our attention on the dynamic behavior of tumors after the second follow-up (six months after radiosurgery). Taking into account that the average time between follow-ups in the clinic is 3 months, for each case we calculated the following three volume measurements from six months post-SRS, that is, t = 6, 9 and 12 months. Volume measurements were calculated as explained in [1]. All cell populations were taken into account and a filled voxel threshold equal to 0.45 was used. After that, we fitted the volumes to the growth law as explained in 'Methods' and calculated the value of the exponent β.

To avoid possible conditioning of the estimate in the choice of time points, the three time instances were taken within the following ranges: $t_0 \in (180, 180 + 15)$ days, $t_1 \in (t_0 + 80, t_0 + 100)$ days and $t_2 \in (t_1 + 80, t_1 + 100)$ days. Then, we estimated β for each combination of t_0, t_1 and t_2, repeating this procedure 20 times. Finally, we obtained the estimated $\hat{\beta}$ value for the corresponding simulated tumor as the median value of all the previously calculated values.

Volumetric dynamics of BM relapses after SRS

With the virtual BMs generated, we studied their volumetric growth dynamics after therapy. Figure S3 shows three examples of these in silico simulations. First column (A, C, E) shows the dynamics of the different cell populations present: proliferating tumor cells, damaged cells, necrotic cells, immune cells and total tumor cells for the three cases. The second column (B, D, F) shows the longitudinal volumetric dynamics of the simulation displayed in the first column. In each case, 20 β growth exponents were calculated as explained in section 1. Additionally, $\hat{\beta}$ median was obtained for each simulation. In two of the cases, sublinear growths ($\hat{\beta} < 1$) were obtained for relapses. These simulations were generated with small or no damage to healthy tissue, i.e, $S_n = 1$ (Figure S3 (A,B)) and $S_n = 0.7$ (Figure S3 (E,F)). On the other hand, when there was a substantial damage to healthy tissue $S_n = 0.1$, the volumetric evolution displayed a superlinear growth ($\hat{\beta} > 1$), as shown in Figure S3 (C,D).

Thus, in order to characterize the volumetric growth post-SRS of the BMs using the scaling exponent, the values of β were calculated for the set of 400 virtual BMs. The results obtained for the first group ($S_n = 1$) are shown in Main Text Fig. 3(f1). The values of β were grouped according to the value of $S_{\hat{f}}$ used in the simulation. Medians and the quartiles of the box plots were mostly below 1, although for small values of $S_{\hat{f}}$ there were a set of outliers with high estimates of β. These exponents described the dynamics of relapsing lesions.

For the second group, which included damage to healthy tissue, there were two behaviors observed in silico. Figure S4 shows the scatter plot of the $\hat{\beta}$ median calculated for the virtual BMs according to the different values of ($S_{\hat{f}}$, S_n) simulated. Values of $\hat{\beta} > 1$ were obtained for cases where SRS eliminates most of the tumor cells (values of $S_{\hat{f}} \leq 0.1$). Here, the volume re-growth was due to the inflammatory component. Otherwise, for larger tumor remnants re-growth simulations (values of $0.1 < S_{\hat{f}} < 1$) the calculated $\hat{\beta}$ exponents were less than 1. This behavior corresponds to a tumor relapse. In addition, we can see in Main Text Fig. 3(f2) the β values calculated for the cases simulated with $0.1 \leq S_n \leq 0.7$ and $S_{\hat{f}} \leq 0.1$. Despite the presented variability, β values obtained were typically greater than 1.

The computational results suggest that β value could be used to distinguish inflammatory response from tumor progression. The ANOVA test for the comparison with the BMs virtual lead to significant differences between inflammatory response group

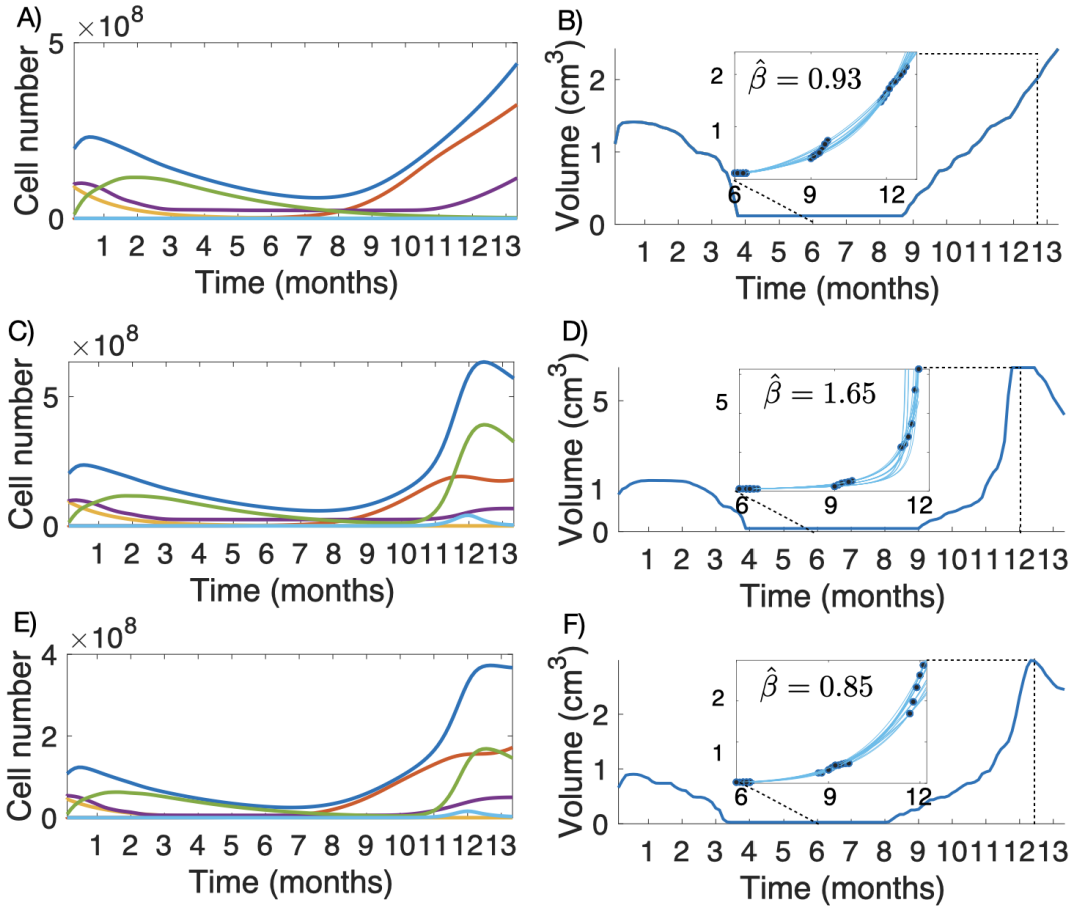

Figure S3 **Longitudinal tumor growth dynamics after SRS**. The first column shows the dynamics of the proliferating cells (red line), damaged cells (orange line), necrotic cells (violet line), immune cells (green line) and total tumor cells (blue line). The second column shows the longitudinal tumor volumetric dynamics. Subplots (**A-B**) correspond with a tumor simulation with no damage to healthy tissue ($S_n = 1$), subplots (**E-F**) correspond with small damage to healthy tissue ($S_n = 0.7$) and subplots (**C-D**) correspond with high damage to healthy tissue $S_n = 0.1$.

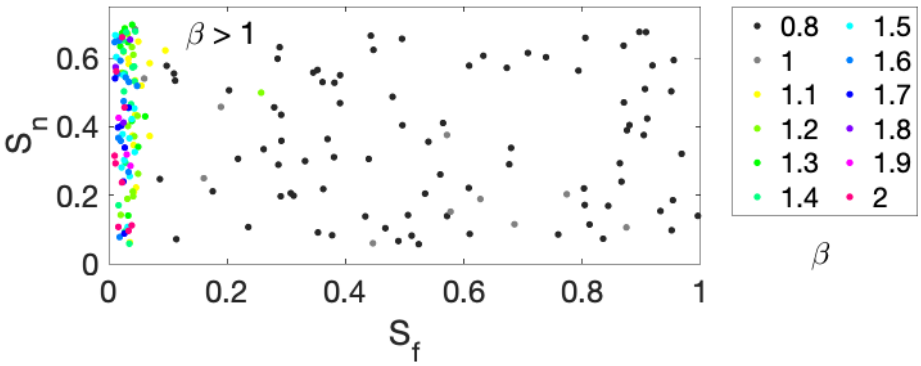

Figure S4 Scatter plot that shows the β median calculated for the virtual BMs which were simulated with different values of $(S_{\hat{f}}, S_n)$. Parameters for this simulation are as in Table S1.

and relapses groups (p=1.85×10^{-12}). Box plots for the different subgroups are shown in Main Text Fig. 3(g). The area under the ROC curve (AUC) in Main Text Fig. 3(h) illustrates the ability of the exponent $\hat{\beta}$ to discriminate between responses groups. We obtained AUC=0.97 and the optimal threshold calculated to maximize the sensitivity and specificity values was $\beta_{threshold} = 1.05$. This means that inflammatory events show faster growth dynamics than relapses.

S2. Sensitivity to small changes in volume when computing beta

Since only three points per patient were available to obtain three parameters, the fitting could be very sensitive to small variations in the data. Those variations in volumetric data could be given either by image segmentation, regardless being performed by the same image expert, and revised by another expert and a radiologist, or by the time between MRIs.

In order to check this fact, a random error smaller or equal to ±5% was added to every volume. The process was performed 200 times for each BM, computing β^* for each set of random errors. The average of the 200 computed β^* was imposed to has a difference smaller than 0.5 when compared with the computed β for the measure volumes, that is to say, $|\beta^*_{av} - \beta| < 0.5$.

Imposing the previous condition, 27 of the 106 BMs used for the study were excluded. The Kruskal-Wallis test was performed to the remaining BMs, and significant differences ($p = 0.0049$) were found when comparing relapsing BMs with the RN group. Having only three time points per BM affects the model fitting and computation of β, however, when sensitive cases are excluded, results agree with the ones found for the whole cohort of BMs, ensuring the strength of the study.

References

[1] Jiménez-Sánchez J. et al., A mesoscopic simulator to uncover heterogeneity and evolutionary dynamics in tumors. *PLoS Comput Biol*. **17(2)** (2021).

[2] Hanahan, D., Weinberg, R.A., The hallmarks of cancer: the next generation. *Cell*. **144(5),** 646-674 (2011).

[3] Yu, C. & Shepard, D. , Treatment planning for stereotactic radiosurgery with photon beams. *Technol Cancer Res Treat*. **2(2),** 93-104 (2003).

[4] Milo, R., Jorgensen, P., Moran, U. & Weber, G., BioNumbers-the database of key numbers in molecular and cell biology. Nucleic Acids Research. *Nucleic Acids Res* **38,** D750–D753 (2009).

[5] Kobets, A.J., Backus, R., Fluss, R., Lee, A., Lasala, P.A., Evaluating the natural growth rate of metastatic cancer to the brain. *Surg Neurol Int*. **11,** 254 (2020).

[6] Leon-Triana, O. et al., Brain metastasis response to stereotactic radio surgery: A mathematical approach. *Mathematics*. **9,** 716 (2021).

[7] He B. et al., Gamma ray-induced glial activation and neuronal loss occur before the delayed onset of brain necrosis. *FASEB J*. **34(10),** 13361-13375 (2020).

[8] Wagner, S., Lanfermann, H., Wohlgemuth, W.A. & Gufler, H. , Effects of effective stereotactic radiosurgery for brain metastases on the adjacent brain parenchyma. *Br J Cancer*. **123(1),** 54-60 (2020).

[9] Askew, K. et al., Coupled proliferation and apoptosis maintain the rapid turnover of microglia in the adult brain. *Cell Rep*. **18(2),** 391-405 (2017).

[10] Davis, B.M., Salinas-Navarro, M., Cordeiro, M.F., Moons, L. & De Groef, L., Characterizing microglia activation: a spatial statistics approach to maximize information extraction. *Sci Rep*. **7(1),**1576 (2017).

[11] Zaer, H. et al. , Radionecrosis and cellular changes in small volume stereotactic brain radiosurgery in a porcine model. *Sci Rep*. **10,** 16223 (2020).

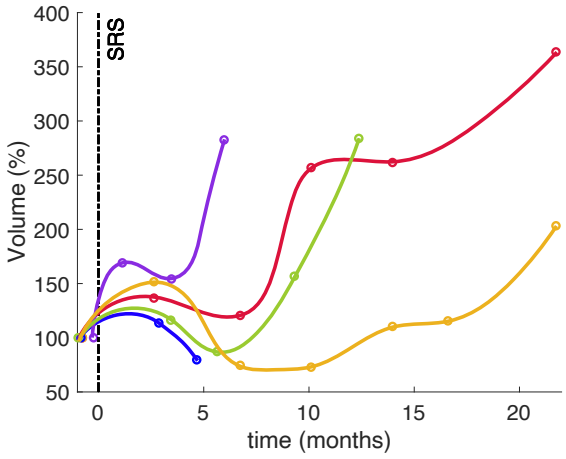

Figure S5 Longitudinal tumor growth dynamics of BMs which display early inflammatory response after SRS. SRS treatment time is marked with a vertical dashed black line and dots are the measured volumes in percentage. Lines give no additional information and are shown only to guide the eye.

$V_0\ (cm^3)$	β_m
0.5	2.7895
1.0	4.1332
1.5	3.7949
2.0	5.0124
2.5	5.9064
3.0	5.8784

Table S2 Mean β values computed for each given initial volume V_0. For each V_0, 500 virtual BM were simulated by model in Eqs. (6) assuming radiation necrosis. Regardless the initial volume, all mean β values were greater than 2.

Chemotherapy type	Number of BMs (percentage)
Ado-trastuzumab emtansine (T-DM1)	8 (16%)
Vinorelbine	7 (14%)
Pemetrexed + carboplatin	4 (8%)
Trastuzumab + vinorelbine	3 (6%)
Erlotinib	3 (6%)
Unknown	3 (6%)
Vemurafenib	2 (4%)
Trastuzuman+lapatinib	2 (4%)
Nivolumab	2 (4%)
Pembrolizumab	2 (4%)
Pemetrexed	2 (4%)
Afatinib	2 (4%)
Lorlatinib	2 (4%)
Nivolumab	1 (2%)
Tamoxifeno+Fulvestrant	1 (2%)
Vinorelbine + carboplatin	1 (2%)
Paclitaxel	1 (2%)
Sorafenib	1 (2%)
CDDP-VP16	1 (2%)
Nivolumab-gemcitabina	1 (2%)
Carboplatin + etoposide + atezolizumab	1 (2%)

Table S3 Chemotherapeutic drugs received by the patients who meet the inclusion criteria and number of BMs of those patients.

Patient characteristics	
Number of patients	77
Number of metastases	106
Age (years) median (range)	56.75 (33-78)
Metastases per patient median (range)	1.63 (1-19)
Sex (Male (M), Female (F)) Percentage (number of patients)	45% M (34), 55% F (41)
Primary cancer Histology	
	Percentage (number of BMs)
NSCLC	60.38% (64)
Breast	26.41% (28)
Melanoma	4.72% (5)
SCLC	5.66% (6)
Others	2.83% (3)
Volumetric parameters	
	mean (range)
Total tumor volume (cm^3)	0.895 (0.003-33.106)
CE volume (cm^3)	0.801 (0.003-28.989)
Necrotic volume (cm^3)	0.025 (0.000-22.800)

Table S4 Summary of patient and BM characteristics, histology and volumetric parameters.

	λ_N ($days^{-1}$)	γ ($days^{-1} \cdot cells^{-1}$)	λ_I ($days^{-1}$)
BM 1	0.0070	6.100e-09	0.07
BM 2	0.0004	1.830e-08	0.07
BM 3	0.0040	1.300e-07	0.07
BM 4	0.00075	1.444e-08	0.07
BM 5	0.0020	1.720e-08	0.07
BM 6	0.0010	1.500e-08	0.07

Table S5 Parameters used for fitting the available longitudinal volumetric data in the patients subgroup with diagnosed Radiation Necrosis by model in Eqs. (6).